Available online at www.sciencedirect.com

ScienceDirect

Procedia Materials Science 8 (2015) 261 – 270

Procedia Materials Science

www.elsevier.com/locate/procedia

International Congress of Science and Technology of Metallurgy and Materials, SAM - CONAMET 2013

Redox Transformation Of Poly(o-aminophenol) (POAP) Film Electrodes Under Continuous Potential Cycling

Ricardo Tucceri[a]

[a]*Instituto de Investigaciones Fisicoquímicas Teóricas y Aplicadas (INIFTA), CONICET, Facultad de Ciencias Exactas (UNLP), Sucursal 4, Casilla de Correo 16, 1900-La Plata, Argentina*

Abstract

The aim of this work was to study the effect of prolonged potentiodynamic cycling (PPC) on the conducting properties of poly(o-aminophenol) (POAP) film electrodes. PPC reduces strongly the electron and ion transport rates at POAP films. Cyclic Voltammetry (CV), Rotating Disc Electrode Voltammetry (RDEV) and Electrochemical Impedance Spectroscopy (EIS) were employed in this study. The attenuation of the voltammetric response of the polymer with the increase in the number of oxidation-reduction cycles allowed one to define a degree of deactivation. RDEV and EIS were employed to obtain dependences of charge-transport and charge-transfer parameters on the degree of deactivation of the polymer. RDEV data were interpreted on the basis of the electron hopping model. Impedance spectra of POAP films in the presence of an electroactive solution containing *p*-benzoquinone (Q) and hydroquinone (HQ) species were analyzed on the basis of an impedance model which considers a uniform and nonporous polymer film and no penetration of redox species into the film from the solution While diffusion coefficients for electron (D_e) and ion (D_i) transport decrease, interfacial resistances related to ion ($R_i^{f|s}$) and electron ($R_{m|f}$, $R_e^{f|s}$) transfer across the different interfaces involved in the metal/polymer film/solution system increase as the degree of deactivation increases. The slower electron transport with the increase in the degree of deactivation was attributed to the increase of the electron hopping distance between redox sites. Transport parameters, such as, $R_i^{f|s}$ and D_i, were associated with proton movements. POAP films maintain their conducting properties almost unaltered for about 500 potential cycles at a scan rate of 0.010 V s^{-1}. However, a loss of conductivity was observed as the number of potential cycles was extended beyond 500.

Selection and peer-review under responsibility of the scientific committee of SAM - CONAMET 2013

Keywords: poly(o-aminophenol) film electrodes; prolonged potential cycling (PPC); deactivation; charge-transport and charge-transfer parameters

* Corresponding author. R. Tucceri, Tel.: +0054-0221-425-7430; fax: +0054-221-425-4642.
E-mail address: rtucce@gmail.com

Selection and peer-review under responsibility of the scientific committee of SAM - CONAMET 2013
doi:10.1016/j.mspro.2015.04.072

1. Introduction

The oxidation of *o*-aminophenol (*o*-AP) on different electrode materials (gold, platinum, carbon, indium-tin oxide, etc.) in aqueous medium was shown to form poly-*o*-aminophenol (POAP) Barbero et al. (1990). *O*-AP can be polymerized electrochemically in acidic, neutral and alkaline solutions. While a conducting film is only formed in acidic media, POAP synthesized in neutral and alkaline media leads to a nonconducting film Tucceri at a. (2013). The charge-transport process at POAP films synthesized in acid medium was mainly studied from the basic research viewpoint employing different electrochemical techniques Levin et al. (2005). POAP synthesized in acidic medium is found to be a useful material to build electrochemical sensors Miras et al. (2003) and electrocatalysts Zhang et al. (1996). Considering the interest in POAP synthesized in acid medium in both basic and applied research, no much attention has been paid to the decay of the electroactivity of POAP caused by its extensive use. The aim of the present work is to study how the charge-transport and charge-transfer parameters of POAP change with PPC.

2. Experimental

A gold rotating disc electrode (RDE) was used as base electrode to deposit POAP films. This gold RDE consisted of a gold rod press-fitted with epoxy resin into a Teflon sleeve so as to leave a 1cm^2 disc area exposed. In order to obtain a more specular gold surface to deposit POAP films, a gold film about 50 nm in thickness was deposited by vacuum evaporation Tucceri et al. (2004) (~ 10^{-7} Torr) on the gold disc. Then, in all experiments carried out in this work, POAP films were deposited on a specular gold film surface. POAP films were grown on these base electrodes following the procedure described by Barbero et al. (1990). In the same way as described by Barbero et al. (1987), POAP films were grown up to an approximate thickness of $\phi_p \sim 60$ nm by using a reduction charge ($Q_{Red,T}$ = 2.8 mC cm^{-2}) *versus* the ellipsometric thickness working curve. These POAP-coated gold film electrodes were then rinsed and transferred to the supporting electrolyte solution (0.4 M $NaClO_4$ + 0.1 M $HClO_4$) free of monomer, where they were stabilized by a continuous potential cycling at a scan rate of 0.01 V s^{-1}. A typical voltammetric response of these films is shown in Fig. 1 (a) (plot (a)). The POAP films maintain this response on potential cycling within the potential range -0.2 V < E < 0.5 V up to 500 cycles. These POAP films are herein called nondeactivated films. A large-area gold grid was used as counterelectrode. All the potentials reported in this work are referred to the SCE.

A series of eight POAP-coated RDE was prepared (see first column in Table 1) and each one of them was successively employed in an individual experiment. That is, each POAP film was subjected to a different number of potential cycles (higher than 500 cycles, see second column in Table 1) within the potential region –0.2 < E < 0.5 V in a deoxygenated supporting electrolyte solution. Then, the corresponding *j*-*E* responses for each one of the eight POAP films were recorded. An attenuation of the voltammetric response was observed for these films when the number of potential cycles was higher than 500 (Fig. 1 (a)). These POAP films are herein called deactivated films. Then, with both nondeactivated and deactivated POAP films, RDEV and *ac* impedance experiments were performed in the presence of a solution containing equimolar concentrations of *p*-benzoquinone (Q) and hydroquinone (HQ) species (0.1 M $HClO_4$ + 0.4 M $NaClO_4$ + 2 x 10^{-3} M Q/HQ). Stationary current-potential curves (*I*-*E*) at different electrode rotation rates, Ω, were recorded. From these curves, cathodic and anodic limiting current *versus* electrode rotation rate (I_{lim} *versus* $\Omega^{1/2}$) dependences were obtained. Also, with nondeactivated and deactivated POAP films, *ac* impedance diagrams at the cathodic current plateaux were obtained for different electrode rotation rates. In some experiments the HQ/Q redox couple concentration in solution was varied.

In CV and RDEV measurements a PAR Model 173 potentiostat and a PAR Model 175 function generator were used. An X1-X2-Y Hewlett-Packard Model 7046 B plotter was used to record *j*-*E* and steady-state current-potential curves *I*-*E*. The electrode rotation speed, Ω, was controlled with homemade equipment that allows one to select a constant Ω in the range 50 rev min^{-1} < Ω < 7000 rev min^{-1}. This was periodically controlled with a digital photo tachometer (Power Instruments Inc., model 891). Impedance spectra were measured following a 30-min application of the steady-state potential ranging from –0.35 V to 0.0 V. Impedance values were determined at seven discrete frequencies per decade with a signal amplitude of 5 mV. The validation of the impedance spectra was done by using Kramers-Kronig transformations. Impedance measurements in the frequency range 0.01 Hz–10 kHz were performed with a PAR 309 system.

AR grade chemicals were used throughout. *O*-aminophenol (Fluka) was purified as described by Barbero et al. (1990). $HClO_4$ and $NaClO_4$ (Merck) were used without further purification. Benzoquinone and hydroquinone (Merck) were also used without purification. The solutions were prepared with water purified using a Millipore Milli-Q system.

3. Results and discussion

3.1. Voltammetric responses of nondeactivated and deactivated POAP films

The voltammetric response corresponding to a nondeactivated POAP film within the potential range comprised between -0.2 V and 0.5 V is shown in Fig. 1 (a) (plot (a)). As was indicated, the POAP film maintains this response with potential cycling within the potential range -0.2 V < E < 0.5 V up to 500 potential cycles (scan rate 0.01 V s^{-1}).

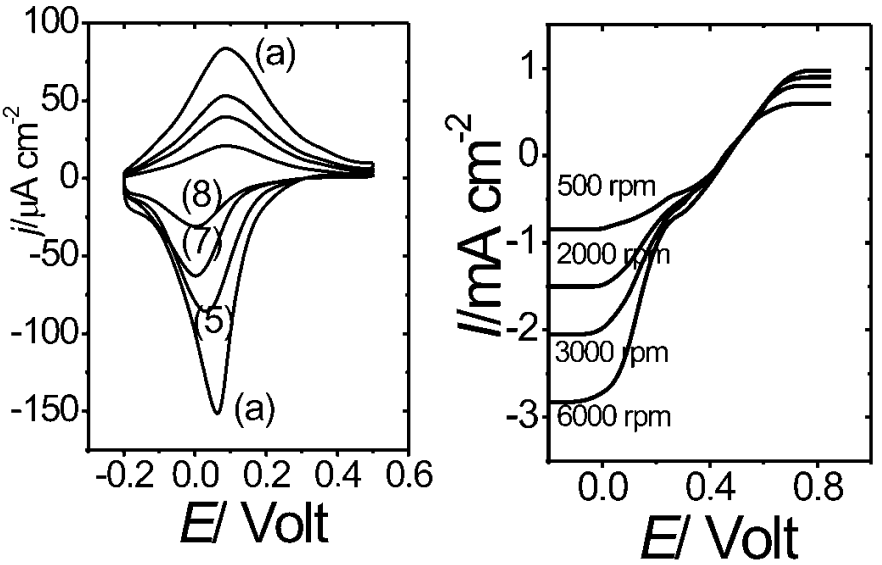

(**a**) (**b**)

Fig. 1. (**a**) Voltammetric (*j*-*E*) responses for a 2.8 mC cm^{-2} (ϕ_p = 60 nm) thick POAP film. (a) A nondeactivated POAP film (θ_c^d = 0). Curves (5), (7) and (8) correspond to films whose degree of deactivation is: θ_c^d = 0.42; θ_c^d = 0.62 and θ_c^d = 0.74, respectively. Electrolyte: 0.1 M $HClO_4$ + 0.4 M $NaClO_4$. Scan rate: ν = 0.01V s^{-1}. (b) Steady-state current-potential (*I*-*E*) curves for different rotation rates (Ω) of the rotating disc electrode. A nondeactivated POAP film. Ω Values are indicated in the figure. Film thickness: 60 nm. Electrolyte: 0.1 M $HClO_4$ + 0.4 M $NaClO_4$+ 2 x 10^{-3} M(HQ/Q).

However, after a higher number of potential cycles this response start to change. Figure 1 (a) compares the *j*-*E* responses of a nondeactivated POAP film (plots (a)) with those of the films (5), (7) and (8) (see first column of Table 1) that were subjected to the corresponding number of potential cycles (> 500) indicated in column 2 of Table 1. The more attenuated voltammetric response observed in Fig. 1 (a), as the number of potential cycles increases indicates a deactivation of the POAP film. In this regard, voltammetric reduction charge values corresponding to the completely reduced POAP films were compared for a nondeactivated film ($Q_{Red,T}$ = 2.8 mC cm^{-2}) and the different deactivated films ($Q_{Red,c}$) indicated in Table 1 (see column 3). Then, a degree of deactivation (column 4 of Table 1) was defined as

$$\theta_c^d = 1 - (Q_{Red,c}/Q_{Red,T}) \quad (1)$$

$Q_{Red,c}$ is the total reduction charge assessed by integration of the corresponding *j*-*E* response from $E = 0.5$ V towards the negative potential direction for a deactivated film, and $Q_{Red,T} = 2.8$ mC cm^{-2} is the total reduction charge for the nondeactivated film. In this way, for a nondeactivated POAP film (plot (a) in Fig. 1(a)) the degree of deactivation was $\theta_c^d = 0$, taking $Q_{Red,T} = 2.8$ mC cm^{-2} as reference charge. However, values of $\theta_c^d > 0$ are indicative of POAP films that have been deactivated.

Table 1. Effect of the prolonged potential cycling on the voltammetric charge of a POAP film

POAP films	Number of potential cycles	$Q_{Red,c}$/mCcm^{-2}	θ_c^d
1	624	2.58	0.08
2	1248	2.30	0.18
3	1872	2.10	0.25
4	2496	2.85	0.34
5	3120	1.62	0.42
6	3744	1.37	0.51
7	4368	1.06	0.62
8	4992	0.73	0.74

3.2. Rotating disc electrode voltammetry and ac impedance measurements in the presence of a HQ/Q solution

In previous work Bonfranceschi at al. (1999) described RDEV experiments at gold electrodes coated with POAP films, which were carried out to study the diffusion processes of benzoquinone (*Q*) and hydroquinone (*HQ*) species through nondeactivated films. Diffusion-limited currents at $E < 0.0$ V for *Q* reduction and at $E > 0.8$ V for *HQ* oxidation were observed. While the anodic limiting current corresponds to the oxidation of *HQ* species that penetrate through the polymer film to reach the metal surface, cathodic limiting currents for *Q* reduction are related to a rapid electron-transfer mediation at the POAP|redox active solution interface, which occurs without significant penetration of *Q* into the polymer layer. As we use the theory of Vorotyntsev et al. (1999) to interpret the impedance behavior of POAP films and this theory was developed within the framework of the assumption that the redox active species are only present in the solution phase but not inside the film, and they participate in the interfacial electron exchange with the polymer at the film-solution boundary, only the electrochemical behavior of nondeactivated and deactivated POAP films at negative potential values ($E < 0.0$ V) was considered.

Figure 1 (b) shows stationary current-potential curves (*I*-*E*) at different electrode rotation rates, Ω, for a nondeactivated POAP film contacting a 0.1 M $HClO_4$ + 0.4 M $NaClO_4$ + 2 x 10^{-3} M Q/HQ solution. (*I*-*E*) curves at different Ω values were also obtained for each one of the deactivated POAP films indicated in Table 1. For instance, Fig. 2 (a) shows this representation for a POAP film with $\theta_c^d = 0.51$. As can be seen by comparing Figs. 1 (b) and 2 (a), at each electrode rotation rate, both anodic and cathodic limiting currents for a deactivated POAP film are lower than those for a nondeactivated one. Also, after a given electrode rotation rate, which depends on the degree of deactivation, the cathodic limiting current for a deactivated film becomes independent of this variable. $I_{lim,c}$ *versus* $\Omega^{1/2}$ dependences at potential values $E < 0.0$ V for both nondeactivated and deactivated POAP films are shown in Fig. 2 (b). For a nondeactivated POAP film a linear $I_{lim,c}$ *versus* $\Omega^{1/2}$ dependence, which follows the Levich equation, is obtained within a wide range of Ω values. However, for POAP films that have been deactivated, after a certain Ω value, a constant cathodic limiting current value, $I_{lim,c}$, independent of Ω is achieved. Also, it is observed that the transition at which the cathodic limiting current becomes independent of Ω occurs at lower Ω values as the degree of deactivation increases.

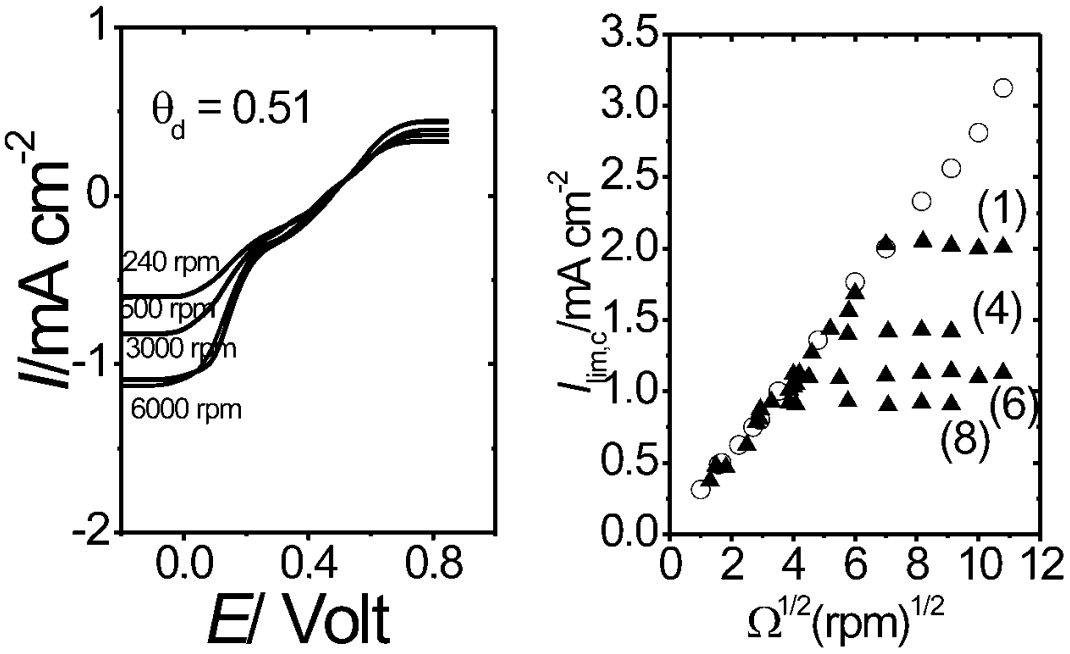

(a) (b)

Fig. 2. (**a**) Steady-state current-potential (*I-E*) curves for different rotation rates (Ω) of the rotating disc electrode. A deactivated POAP film (θ_c^d = 0.51). Ω Values are indicated in the figure. Film thickness: 60 nm. Electrolyte: 0.1 M $HClO_4$ + 0.4 M $NaClO_4$+ 2 x 10^{-3} M(HQ/Q). (b) Levich representations $I_{lim,c}$ *versus* $\Omega^{½}$ for POAP films contacting a 0.1 M $HClO_4$ + 0.4 M $NaClO_4$.+ 2 x 10^{-3} M (HQ/Q) solution. (O) A nondeactivated POAP film. (1), (4), (6) and (8) correspond to the four films indicated in Table 1.

The explanation of this effect can be given in terms of the electron hopping model described by Deslouis et al. (1992). Limiting current values at which Ilim,c (= Ie) becomes constant were considered as a representation of the maximum flux of electrons confined in the polymer, according to Eq. (2) (Deslouis et al. (1992)

$$I_e = n\,F\,A\,D_e\,c/\phi_p \qquad (2)$$

In Eq. (2), c is the concentration of redox sites of the polymer and ϕp the polymer film thickness. De represents a measure of the electron hopping rate and n expresses the numbers (fractions) of unit charges per monomer unit of the polymer. A is the electrode area and F the Faraday's constant. Experimental Ie values, corresponding to each one of the eight deactivated POAP films contacting a 2 x 10-3 M HQ/Q solution, were extracted from the cathodic plateau. As can be seen from Fig. 2 (b), Ie decreases with increasing θcd. In this regard, such a constant value of the current (Ie) at a given Ω value for deactivated POAP films can be related to a slow electron transport across the POAP film to mediate in the electron-transfer reaction at the polymer|solution interface, as compared with a nondeactivated POAP film. As one increases the flux of Q (increase of Ω) from the bulk solution, then if the flux exceeds the supply of electrons from the electrode through the polymer to the electrolyte interface, the rate-limiting step will shift from the limiting transport of Q to the limiting transport of the charge through the polymer. In order to verify this limiting charge-transport process across the POAP film, the HQ/Q concentration in solution was varied. It is found that despite the Ilim,c versus Ω1/2 slope increase with the increase of the HQ/Q concentration, the constant current value for a given deactivated film remains unchanged. According to Eq. (2), the slower electron transport in deactivated films, as compared with nondeactivated ones, could be attributed to a decrease of De. By employing the experimental Ie values and the parameter values c = 4.7 M, A = 1 cm2, n = 0.44 and ϕp = 60 nm in Eq. (2), one obtains a decrease of De from 6.01 x 10-11 to 2.76 x 10-11 cm2 s-1 for a relative increase of θc from 0.08 to 0.74.

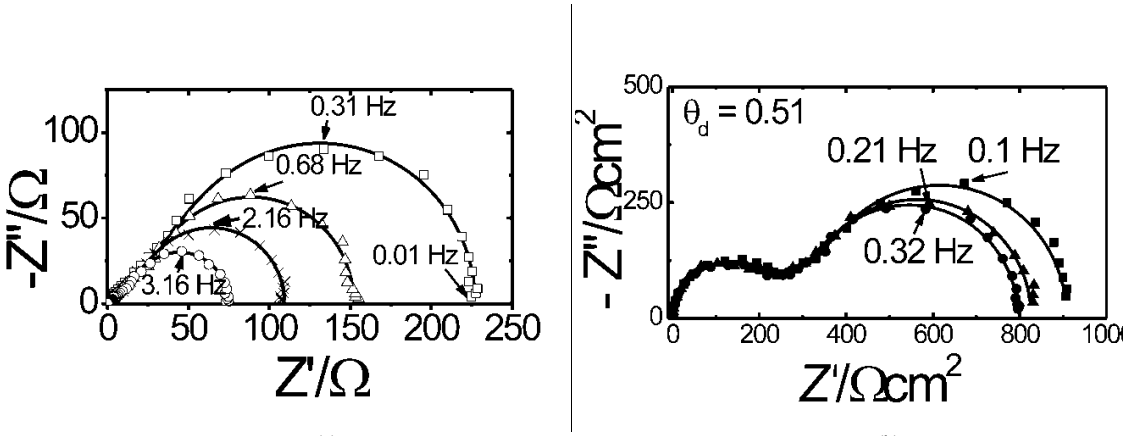

(a) (b)

Fig. 3. (**a**) *Ac* impedance diagrams in the Nyquist coordinates (-*Z*'' *versus Z*) obtained at E = -0.2 V for a nondeactivated POAP film. The different diagrams correspond to different electrode rotation rates, Ω: (□) 100 rpm; (Δ) 200 rpm; (X) 300 rpm; (O) 600 rpm. Electrolyte: 0.1 M $HClO_4$ + 0.4 M $NaClO_4$ + 2 x 10^{-3} M (HQ/Q) solution. Discrete points are experimental data and continuous lines represent the fitting by using the theory described by Vorotyntsev et al. (1999). (**b**) *Ac* Impedance diagrams in the Nyquist coordinates (-*Z*'' *versus Z*) obtained at E = -0.2 V for a deactivated POAP film, θ_c^d = 0.51. The different diagrams correspond to different electrode rotation rates, Ω: (■) 1000 rpm ; (▲) 1500 rpm; (●) 3000 rpm. Electrolyte: 0.1 M $HClO_4$ + 0.4 M $NaClO_4$ + 2 x 10^{-3} M (HQ/Q) solution. Discrete points are experimental data and continuous lines represent the fitting by using the theory described by Vorotyntsev et al (1999).

The electron diffusion coefficient, D_e, in electroactive materials has been expressed by Chidsey et al. (1986) in terms of the mean distance between adjacent active redox sites, according to $D_e = (a^2k)$, where k is the intermolecular electron-transfer rate constant and a is the mean distance between two adjacent redox sites. The hopping rate, k, exhibits an exponential dependence on a, through the energy $-U(x+a)$ of a state with an electron in the position x along the current direction. In this respect, a k decrease should be expected as the hopping distance a increases. The decrease of D_e obtained from Eq. (2) could be attributed to an increase of the hopping distance between remnant active redox sites after deactivation.

Impedance measurements were also performed with nondeactivated and deactivated POAP films contacting a 0.1 M $HClO_4$ + 0.4 M $NaClO_4$ + 2 x 10^{-3} M (Q/HQ) solution at potential values E < 0.0 V. Nyquist diagrams at different electrode rotation rates for a nondeactivated POAP film are shown in Fig. 3 (a). A Warburg region at high frequency, followed by a semicircle, is observed in the impedance diagrams of a nondeactivated film. Impedance diagrams of each one of the eight deactivated POAP films indicated in Table 1 exhibit two loops (Fig. 3 (b)). While the loop at low frequency is Ω dependent, the high-frequency semicircle is independent of this variable. However, the size of the high-frequency semicircle depends on the degree of deactivation. In this regard, at a given Ω value, the higher the θ_c^d value is, the greater the high-frequency semicircle becomes.

3.3. Interpretation of ac impedance diagrams

On the basis of the experimental arrangement used, i.e., a gold disc electrode of low surface roughness (high specularity) after deposition of a thin gold film by evaporation coated with a thick POAP film, the system could be considered as a good enough approximation to a uniform polymer layer deposited on a smooth electrode surface to apply a homogeneous electrochemical impedance model in the interpretation of experimental *ac* impedance diagrams. It is well-known that thin metal films obtained by evaporation (low rate of evaporation) exhibit specular surfaces with a relatively low amount of defects as compared with a massive metal surface. The specularity of a metal film surface is represented by its specularity parameter, p as described by Tucceri et al. (2004). Our gold films are prepared at low evaporation rates and they show a specularity parameter near 0.91.

With regard to the thickness of the POAP film, it was demonstrated by Bonfranceschi et al. (1999) that POAP deposition on a rotating gold disc starts with the formation of a rather porous structure whereas dense structures are formed later on as the polymer thickness increases. SEM images and permeation rate measurements reported by Bonfranceschi et al. (1999) show that thick POAP films (thickness higher than 50 nm thickness) are uniform and

compact enough to restrain the physical diffusion of species through the film. Also, resistance measurements on POAP-coated gold film electrodes described by Tucceri et al. (2004) demonstrate the POAP coverage higher than 0.8 mC cm^{-2} (60 nm) are sufficiently compact at the gold-POAP interface to prevent the specific adsorption of anions and cations proceeding from the external electrolyte solution on the gold film surface.

Then, as was indicated, the general theory of *ac* impedance described by Vorotyntsev et al. (1999) was employed to interpret experimental impedance data of this modified electrode system. As in the present case one has the modified electrode geometry with a redox active electrolyte solution (m|film|es), Eq. (3) must be applied

$$Z_{m|film|es} = R_{m|f} + R_f + R_s + [Z_e^{f|s} R_i^{f|s} + W_f Z_{12}^{m}] (Z_e^{f|s} + R_i^{f|s} + 2 W_f \coth 2\nu)^{-1} \quad (3)$$

where

$$Z_{12}^{m} = Z_e^{f|s} [\coth \nu + (t_e - t_i)^2 \tanh \nu] + R_i^{f|s} 4t_i^2 \tanh \nu + W_f 4t_i^2 \quad (4)$$

In Eqs. (3) and (4):

$\nu = [(j\omega\phi_p^2)/4D]^{1/2}$ is a dimensionless function of the frequency ω, ϕ_p is the film thickness, D is the binary electron-ion diffusion coefficient, and t_i and t_e are the migration (high frequency) bulk-film transference numbers for anions and electrons, respectively. D is defined as $D = 2D_iD_e(D_e+D_i)^{-1}$ and $t_{i,e} = D_{i,e}(D_e+D_i)^{-1}$, where D_e and D_i are the diffusion coefficients for the electrons and ion species, respectively.

$W_f = [\nu/j\omega\phi_pC_p] = \Delta R_f/\nu$ is a Warburg impedance for the electron-ion transport inside the polymer film. ΔR_f ($=\phi_p/4DC_p$) is the amplitude of the Warburg impedance inside the film, and C_p is the redox capacitance per unit volume.

R_f ($=\phi_p/\kappa$) is the high-frequency bulk-film resistance, R_s the ohmic resistance of the bulk solution (κ is the high-frequency bulk conductivity of the film), $R_{m|f}$ is the metal|film interfacial electron-transfer resistance, and $R_i^{f|s}$ is the film|solution interfacial ion-transfer resistance.

$Z_e^{f|s} = (R_e^{f|s} + W_s)$ is the electronic impedance, where $R_e^{f|s}$ is the interfacial electron-transfer resistance at the film|solution interface, and W_s is the convective diffusion impedance of redox species in solution, which contains the bulk concentrations of ox(red) forms, c_{ox}(c_{red}), and their diffusion coefficients inside the solution, D_{ox}(D_{red}). Also, it contains the Nernst layer thickness, δ.

$R_e^{f|s}$ is defined as

$$R_e^{f|s} = RT (nF^2 k_o c_{red})^{-1} \quad (5)$$

where k_o is the rate constant of the reaction between the film and the redox active forms in solution.

3.4. Dependences of the different charge-transport and charge-transfer parameters on the degree of deactivation

Continuous lines on the impedance diagrams shown from Figs. 3 (a) and (b) are simulated curves calculated by using Eq. (3). A good fitting was observed for the different impedance diagrams. The fitting procedure by using Eq. (3) was based on the CNLS (Complex Nonlinear Squares) method. A rigorous fitting procedure was performed. Six replicate measurements for each degree of deactivation were carried out, and the error structure was assessed following the method recommended by Agarwal et al. (1995). In the simulations the number of transferred electrons, n, was assumed to be 0.44, and diffusion coefficient values of the redox species (Q and HQ) were considered equal, $D_{ox,red}$ = 1.5 x 10^{-5} cm^2 s^{-1}. Also, the bulk concentrations of the redox substrate species were considered equal ($c_{ox} = c_{red}$ = 2 x 10^{-6} mol cm^{-3}). The polymer thickness was considered as ϕ_p = 60 nm. The value of the total redox site concentration of POAP was considered as c_o = 4.7 x 10^{-3} mol cm^{-3}. The parameters contained in Eq. (3) ($R_{m|f}$, $R_i^{f|s}$, $R_e^{f|s}$, C_p, D_e and D_i) were calculated from the experimental impedance data by the fitting procedure described above. The first three parameters ($R_{m|f}$, $R_i^{f|s}$ and $R_e^{f|s}$) were varied without restraints during the fitting. However, some reference values were considered for C_p, D_e and D_i. For the nondeactivated POAP film thickness used in this work (ϕ_p = 60 nm) and solution pH = 1, D_e and D_i values were allowed to vary within the range 10^{-7}-10^{-}

^{11} cm^2 s^{-1}, in such a way that diffusion coefficient values lower than 10^{-11} were considered unrealistic for these thick films. Concerning C_p, reference values were extracted from experimental -Z" *versus* ω^{-1} slopes of impedance diagrams at sufficiently low frequency (in the absence of the redox substrate in solution). A contribution of the interfacial capacitance, C_H, also considered as a fitting parameter, was included in order to represent the actual impedance diagrams from the calculated ones.

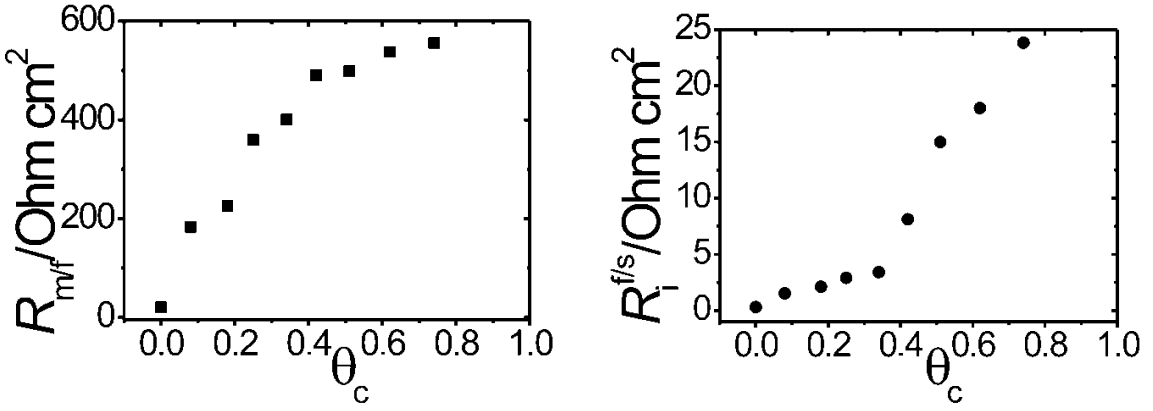

Fig. 4. (a) Metal-polymer interfacial electron-transfer resistance ($R_{m/f}$) as a function of θ_c^d. (b) Polymer-solution interfacial ion-transfer resistance ($R_i^{f/s}$) as a function of θ_c^d. Electrolyte: 0.1 M $HClO_4$ + 0.4 M $NaClO_4$ + 2 x 10^{-3} M (HQ/Q) solution.

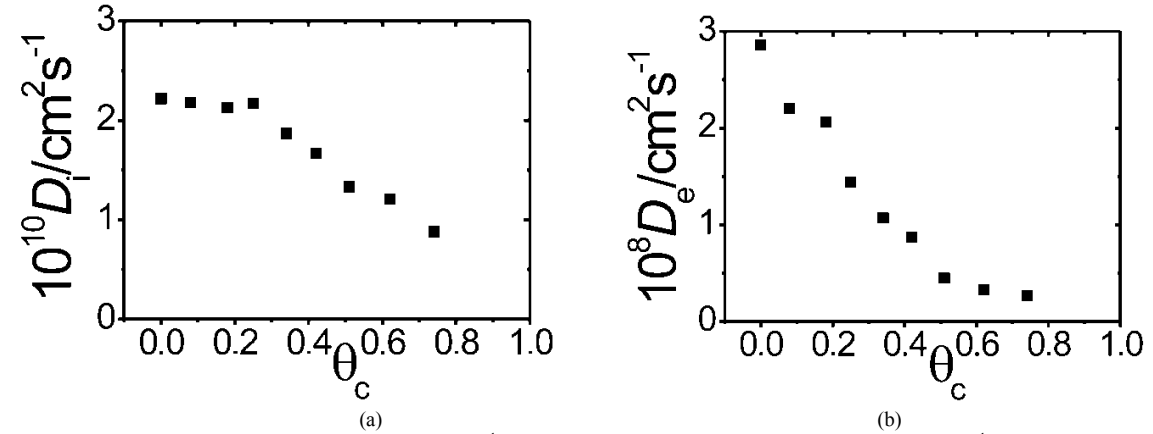

Fig. 5. (a) Ion diffusion coefficient (D_i) as a function of θ_c^d. (b) Electron diffusion coefficient (D_e) as a function of θ_c^d. Electrolyte: 0.1 M $HClO_4$ + 0.4 M $NaClO_4$ + 2 x 10^{-3} M (HQ/Q) solution.

Wit regard to C_p *versus* θ_c dependence, starting from a value of about 27 F cm^{-3}, for a nondeactivated film, a nearly linear decrease of C_p with increasing θ_c^d is observed. This decrease is consistent with the continuous attenuation of the voltammetric response as the degree of deactivation increases. $R_{m|f}$ and $R_i^{f|s}$ on θ_c^d dependences are shown in Figs. 4 (a) and (b), respectively. $R_i^{f|s}$ as a function of θ_c^d exhibits a different feature as compared with $R_{m|f}$. That is, while $R_{m|f}$ seems to change continuously within the whole θ_c^d range, $R_i^{f|s}$ firstly exhibits a slight increase within the range $0 < \theta_c^d < 0.35$ and then, a strong increase is observed within the range $0.35 < \theta_c^d < 0.74$. Also, the magnitude of $R_{m|f}$ and $R_i^{f|s}$ change within the whole θ_c^d range is different. $R_i^{f|s}$ change is around one order of magnitude lower than $R_{m|f}$ change. This difference could indicate that the high-frequency semicircle on impedance diagrams (Fig. 3) is mainly determined by $R_{m|f}$. The increase of interfacial $R_{m|f}$ resistance could be due to an increasing number of inactive sites at the metal|polymer interface with the increase of deactivation.

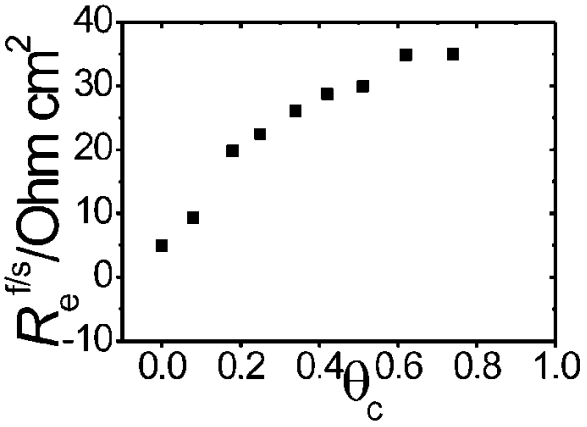

Fig. 6. Interfacial electron-transfer resistance ($R_e^{f/s}$) as a function of θ_c^d. Electrolyte: 0.1 M $HClO_4$ + 0.4 M $NaClO_4$ + 2 x 10^{-3} M (HQ/Q) solution.

Ion and electron diffusion coefficients *versus* θ_c^d dependences are shown in Figs. 5 (a) and (b), respectively. Both diffusion coefficients decrease as θ_c^d increases. As was proposed from RDEV data, the decrease of D_e with the increase of θ_c^d could be attributed to an increase of the hopping distance between remnant redox active sites after polymer deactivation. D_e values are nearly two orders of magnitude higher than D_i values. It is possible that electron hopping controls the charge-transport process at a POAP film in its oxidized state, where the polymer is swollen, which facilitates ion transport. However, in the present work, relative diffusion coefficient values ($D_e > D_i$) refer to the reduced state of POAP. The Vorotyntsev's model (1999) gives D_e values near three orders of magnitude higher than D_e values extracted from RDEV. Another interesting difference between D_e and D_i *versus* θ_c^d dependences can be observed by comparing Fig. 5 (a) and (b). While D_i is reduced one half in going from $\theta_c^d \sim 0$ to $\theta_c^d \sim 0.74$, D_e is reduced more than six times. This would mean that although ion motion always controls the charge-transport process at POAP films, the influence of the electron motion on the whole charge-transport process becomes more pronounced at a high degree of deactivation. With regard to D_e and D_i *versus* θ_c^d dependences, while a continuous decrease is observed for D_e within the whole θ_c^d range, a break around $\theta_c^d \sim 0.35$ seems to be observed in the D_i *versus* θ_c^d dependence. The break also becomes evident in the $R_i^{f|s}$ *versus* θ_c^d dependence (Fig. 4 (b)). Probe beam deflection measurements reported by Salvagione et al. (2005) suggest that while protons and anions are exchanged during POAP oxidation, insertion of protons is the dominant process during the POAP reduction process. Also, impedance measurements reported by Levin et al. (2005) indicate that POAP is only doped with hydrogen ions and the effect of anions is negligible. Then, it is possible that both parameters $R_i^{f|s}$ and D_i are related to proton movements across the POAP|solution interface and inside the polymer film, respectively, rather than to anion transport. Concerning the proton movement into POAP films, the existence of two forms (mobile and bound) of hydrogen ions in the bulk film has been proposed by Levin et al. (2005). It was suggested that in polymers derived from aromatic amines, hydrogen ions could be constrained by nitrogen atoms of polymer chains and do not contribute to the electrical conductance of the film, and another part of such constrained groups is able to dissociate producing the mobile form of hydrogen, which provides the film conductance. In other words, besides mobile protons, some traps for hydrogen ions within the bulk of the film may be present, which provides the binding of these protons with polymer film fragments. In this regard, the slight increase in the $R_i^{f|s}$ *versus* θ_c^d (the slight decrease in the D_i *versus* θ_c^d) dependence within the range $0 < \theta_c^d < 0.35$ could be due to the inhibition of traps for hydrogen ions, which only causes a small ion conductivity change. However, the strong $R_i^{f|s}$ increase (more pronounced D_i decrease) for $\theta_c^d > 0.35$ could be attributed to the inhibition of nitrogen-containing groups that provide the binding of hydrogen ions and at the same time are able to dissociate and give the mobile form of hydrogen that markedly contributes to the polymer conductivity.

$R_e^{f|s}$ values were extracted from Eq. (5) using k_o as fitting parameter ($0.01 < k_o < 100$ cm s^{-1}). The feature of $R_e^{f/s}$ *versus* θ_c^d dependence is similar to $R_{m/f}$ *versus* θ_c^d dependence (Fig. 6). However, the $R_e^{f|s}$ values are around one order of magnitude lower than $R_{m/f}$ values. Also, it is interesting to note that the $R_e^{f|s}$ change is higher than the $R_i^{f|s}$

change, particularly at low θ_e^d values. Then, the PPC seems to affect more strongly the polymer|solution interfacial electron-transfer resistance, $R_e^{f|s}$, as compared with the polymer|solution interfacial ion-transfer resistance $R_i^{f|s}$. The increase of interfacial $R_e^{f|s}$ resistance could be due to an increasing number of inactive sites at the polymer|solution interface with the increase of deactivation.

4. Conclusions

In this work it is demonstrated that poly(o-aminophenol) films maintain their conducting properties unaltered for about 500 potential cycles within the potential range -0.2 < E < 0.5 V (SCE) at a scan rate of 0.010 V s^{-1}. However, a loss of conductivity was observed as the number of potential cycles was extended beyond 500. An attenuation of the voltammetric response of POAP is observed with prolonged potential cycling. While electron (D_e) and ion (D_i) diffusion coefficients decrease, interfacial resistances ($R_{m|f}$, $R_i^{f|s}$, $R_e^{f|s}$) increase as the degree of deactivation of the polymer increases. The slower electron transport with the increase in the degree of deactivation was attributed to the increase of the electron hopping distance between redox sites, While parameters representing electron motion extracted from RDEV and impedance measurements seem to change continuously within the whole range of deactivation degree, parameters representing the ion transport show a break at a degree of deactivation of about 0.35. This characteristic of the ion transport at POAP was associated with the existence of two forms of hydrogen ions in the POAP film.

Acknowledgements

The author gratefully acknowledges the Consejo Nacional de Investigaciones Científicas y Técnicas (CONICET) and also the Facultad de Ciencias Exactas, National University of La Plata (UNLP).

References

Agarwal, P., Crisalle, O.D., Orazem, M.E., García-Rubio, L.H., 1995. Application of measurement models to impedance spectroscopy. II. Determination of the stochastic contribution to the error structure, J. Electrochem. Soc. 142, 4149-4158.

Barbero, C., Silber, J.J., Sereno, L., 1990. Electrochemical properties of poly(o-aminophenol) modified electrodes in aqueous acid solutions, J. Electroanal. Chem. 291, 81-101.

Barbero, C., Zerbino, J., Sereno, L., Posadas, D., 1987. Optical Properties of Electropolymerized *Ortho*aminophenol, Electrochim. Acta, 32, 693-697.

Bonfranceschi, A., Pérez Córdoba, A., Keunchkarian, S., Zapata, S., Tucceri, R., 1999, Transport across poly(*o*-aminophenol) modified electrodes in contact with media containing redox active couples. A study using rotating disc electrode voltammetry. J. Electroanal. Chem. 477 ,1-13.

Chidsey, Ch.E.D., Murray, R.W., 1986. Redox capacity and direct current electron conductivity in electroactive materials, J. Phys. Chem. 90, 1479-1484.

Deslouis, C., Tribollet, B., 1992. In: Gerischer, H., Tobias C. (Eds.), Advances in Electrochemical Science and Engineering, vol. 2, VCH Publishers, New York, USA, pp. 205.

Levin, O., Kondratiev, V., Malev, V., 2005. Charge transfer processes at poly-*o*-phenylenediamine and poly-o-aminophenol films. Electrochim. Acta 50, 1573-1585.

Miras, M.C., Badano, A., Bruno, M.M., Barbero, C., 2003. Nitric oxide electrochemical sensors based on hybrid films of conducting polymers and metal phtalocyanines, Portugaliae Electrochimica Acta, 21, 235-243.

Salavagione, H.J., Arias-Padilla, J., Pérez, J.M., Vázquez, J.L., Morallón, E., Miras, M.C., Barbero, C., 2005. Study of the resdox mechanism of poly(o-aminophenol) using in-situ techniques: evidence oftwo redox processes, J. Electroanal Chem. 576, 139-145.

Tucceri, R. 2004. A review about the surface resistance technique in electrochemistry. Surface Science Reports, 56, 85-157.

Tucceri, R., Arnal, P.M., Scian, A.N., 2013. Poly(o-aminophenol) film electrodes. Synthesis and characterization. Formation mechanisms. A review article. Canadian Journal of Chemistry, 91, 91-112.

Vorotyntsev, M.A., Deslouis, C., Musiani, M.M., Tribollet, B., Aoki, K., 1999. Transport across an electroactive polymer film in contact with media allowing both ionic and electronic interfacial exchange, Electrochim. Acta 44, 2105-2115.

Zhang, A.Q., Cui, C.Q., Lee, J.Y. 1996. Metal-polymer interaction in the Ag^+/poly-*o*-aminophenol system, J. of Electroanal. Chem., 413, 143-151.